

**INAF**



**ISTITUTO NAZIONALE DI ASTROFISICA**  
NATIONAL INSTITUTE FOR ASTROPHYSICS

# **ISTITUTO DI RADIOASTRONOMIA**

**Rapporto Interno n.383/06**

## **Optical performances of thin and composite vacuum windows**

*V. Natale, R. Nesti*

### Summary

Two computer procedures based on analytical methods to compute the optical performances of both thin single layer and multilayer dielectrics are presented.

# Contents

<b>1</b>	<b>Introduction</b>	<b>1</b>
<b>2</b>	<b>Wave propagation in dielectric</b>	<b>1</b>
2.1	Homogeneous dielectric film . . . . .	2
2.2	Multilayer and composite materials . . . . .	3
<b>3</b>	<b>Optical performances of multilayer</b>	<b>7</b>
<b>4</b>	<b>Conclusions</b>	<b>9</b>
	<b>References</b>	<b>10</b>
	<b>Appendix</b>	<b>11</b>
<b>A</b>	<b>Derivation of <math>n</math> and <math>\tau</math> from <math>\epsilon</math> and <math>\tan \delta</math></b>	<b>11</b>
<b>B</b>	<b>Mechanical and electrical properties</b>	<b>12</b>

# 1 Introduction

One of the key component of a cooled receiver (coherent or incoherent) for long wavelength, approximately for wavelength longer than about 100 microns is the vacuum windows and the associated infrared filtering. The main performances required to a vacuum window are low reflectivity and high transmission in the frequency band to be detected and, possibly, a quite large rejection to infrared in order to decrease the radiative thermal load on the cryogenerator. Finally, window materials must be able to resist environmental adverse conditions, like, for instance, abrasion caused by flying dust, intense solar radiation, salt water and corrosive gases in the atmosphere, to which prime focus receivers are normally exposed. As a result of the above constraints, the optimal solution for large vacuum windows will require a careful trade-off between the mechanical, optical and chemical characteristics of available materials. A huge number of papers exist collecting optical data [2, 5, 8, 12, 16, 15] on materials, including composite, suitable for vacuum windows of moderate diameters (10 - 20 cm). For larger diameters the problem complexity increases since, in order to achieve good performances over a large bandwidth and to avoid hazards of window rupture, one is forced to use multilayer structures. It is longtime that different kind of multilayer techniques, derived directly from the well known matching technique in the electromagnetic theory, have been proposed to reduce the vacuum window reflectivity in both the infrared [18] and the millimetric and submillimetric regions [17]. For instance in the long millimetric region, a large window can be made by a thin ( $0.01 \lambda$ ) dielectric layer which ensure the vacuum tightness together with thicker rigid expanded materials, like for example Styrodur [23] or Rohacell [24], whose electromagnetic losses due the reflection and absorption is very small. More recently multilayers have been proposed as very low loss vacuum windows for the 3 mm and 1.1 mm Alma receivers [11] and for a 1.1 mm band half-wave plate [14].

In this report we discuss only the electromagnetic performances of the vacuum windows. In Sec. 2 techniques for the analysis of reflection, transmission and absorption in lossy dielectrics, including stacks of different materials, are presented. Simulation data for different combinations of dielectrics are given in Sec. 3. In Appendix A the relationship between e.m. quantities ( $\epsilon_r$ ,  $\tan \delta$ ) and optical quantities (complex refraction index  $\hat{n}$ , absorption coefficient) are derived. Finally in Appendix B mechanical and electrical data for some dielectrics are reported.

## 2 Wave propagation in dielectric

The problem of the electromagnetic wave propagation in dielectric films or composite structures has been tackled by several authors in different areas (the list is however by no means complete) like the study of high resolution multiple beams spectrometers as, for instance, the Fabry-Perot interferometer [7], the antireflection coating of optical components [9], the heath reflecting mirrors [3], etc.

In this Section the main results for single layer films and for composite structures in free space are given.

## 2.1 Homogeneous dielectric film

The reflection  $\mathcal{R}$  and transmission  $\mathcal{T}$  coefficients for a plane wave incident at an angle  $\theta$  on a homogeneous dielectric film in free space (as shown in Fig. 1) can be computed mainly in two ways: a) by summing up with the correct phases all the multiple reflections taking place in the film [7] or b) by solving the well-known boundary value problem [6].

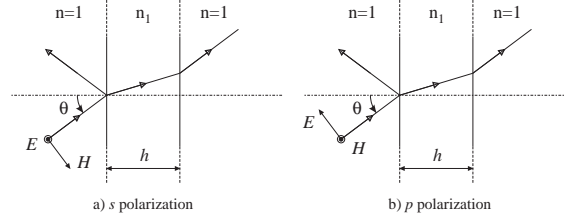


Figure 1: Sketch of the problem of a plane wave incidence on a dielectric layer: a) perpendicular or *s* polarization, b) parallel or *p* polarization

Among the large number of explicit formulations for  $\mathcal{R}$  and  $\mathcal{T}$ , taking into account the complex relative permittivity  $\hat{\epsilon}$  and the angle of incidence, here are reported those given by [19]:

$$\mathcal{T} = \frac{(1 - \hat{r}^2) e^{-j(\beta_1 - \beta_0)h}}{1 - \hat{r}^2 e^{-2j\beta_1 h}} \quad \mathcal{R} = \frac{\hat{r}(1 - e^{-2j\beta_1 h}) e^{2j\beta_0 h}}{1 - \hat{r}^2 e^{-2j\beta_1 h}}$$

where

$$\beta_1 = \frac{2\pi}{\lambda_0} \sqrt{\hat{\epsilon}_1 - \sin^2 \theta} \quad \beta_0 = \frac{2\pi}{\lambda_0} \cos \theta \quad \hat{\epsilon}_1 = \epsilon_r (1 - j \tan \delta)$$

$\theta$  is the angle of incidence,  $\epsilon_r$  and  $\tan \delta$  the e.m. properties of the material,  $\lambda_0$  the free-space wavelength,  $h$  the slab thickness and the appropriate complex Fresnel coefficient  $\hat{r} = \hat{r}_{\parallel}$  or  $\hat{r} = \hat{r}_{\perp}$  depending on the polarization. The Fresnel coefficients, in terms of  $\beta_1$  and  $\beta_0$ , are:

$$\hat{r} = \hat{r}_{\parallel} = \frac{\beta_1 - \hat{\epsilon}_1 \beta_0}{\beta_1 + \hat{\epsilon}_1 \beta_0} \quad \hat{r} = \hat{r}_{\perp} = \frac{\beta_0 - \beta_1}{\beta_0 + \beta_1}$$

The film reflectivity  $R$  and transmissivity  $T$  are, as usual, given by:

$$R = \mathcal{R} \mathcal{R}^* \quad T = \mathcal{T} \mathcal{T}^*$$

where  $*$  denotes the complex conjugate.

Fig.2 shows the reflectivity and transmissivity of a Teflon film, a low loss material, versus the incidence angle and film thickness. It may be worthwhile to note the quite strong different dependance of  $R$  and  $T$  on the wave polarization, parallel (*p* or TM waves) or perpendicular (*s*, from the german *senkrecht* perpendicular, or TE waves) to the plane of incidence. This effect increase rapidly with the material thickness for incident angles larger than few tens of degrees as is evident in the left panel plots. In the right panels  $R$  and  $T$ , for *p* and *s* waves, versus the normalized optical thickness

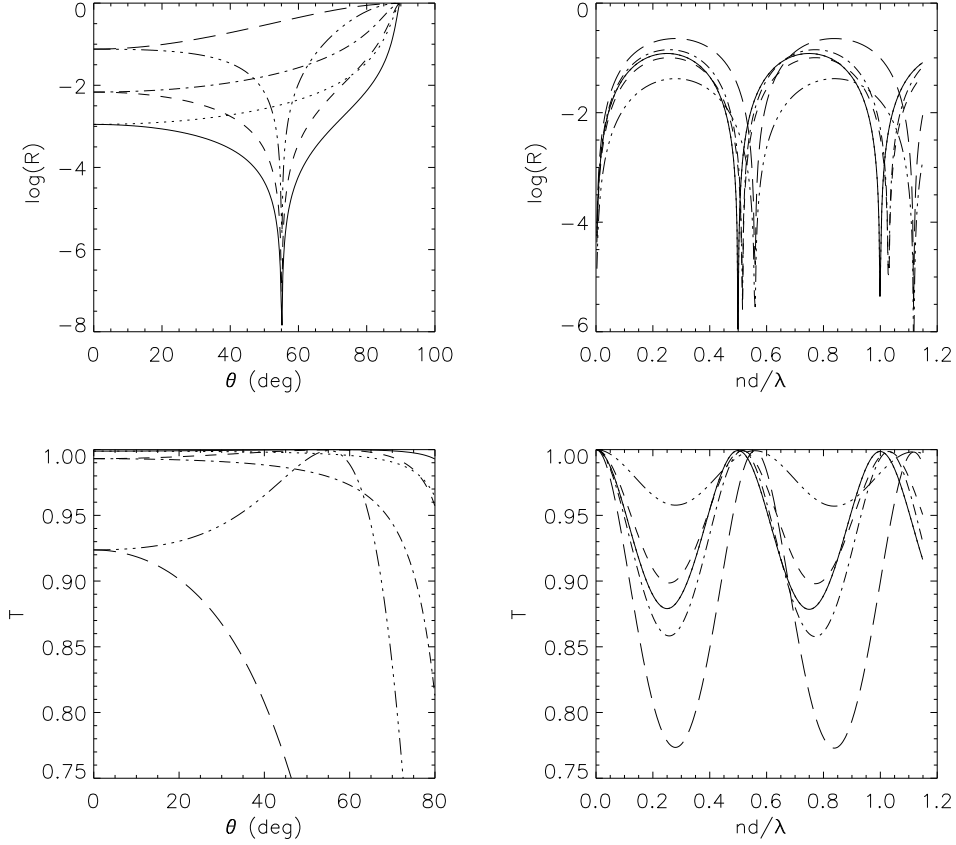


Figure 2: Reflectivity and transmissivity for the Teflon ( $\epsilon_r = 2.065$ ,  $\tan \delta = 0.0002$ ). *Upper left* panel: reflectivity *vs* the incidence angle  $\theta$  for respectively *p* and *s* waves and film thickness:  $h = 0.01\lambda$  (*solid* and *dotted*),  $h = 0.025\lambda$  (*dashed* and *dash-dot*),  $h = 0.25\lambda$  (*dash-dot-dot* and *long dashes*). *Lower left* panel: transmissivity (film thickness and curve types as in upper panel). *Upper right* panel: reflectivity *vs* the film thickness for *p* and *s* waves at  $\theta = 0^\circ$  (*solid* and *dotted*),  $\theta = 20^\circ$  (*dashed* and *dash-dot*),  $\theta = 40^\circ$  (*dash-dot-dot* and *long dashes*). *Lower right* panel: transmissivity (incidence angles and curve types as in the upper panel).

for various incident angles  $\theta$  are shown; obviously for  $\theta = 0$ , there is no difference for different polarization as can be easily verified by inspection of the Fresnel formulae. The ratio  $P = R_p/R_s$  of the reflectivities for *p* and *s* waves is plotted in Fig. 3 for the three film thickness values of Fig. 2; this ratio depends on the incident angle and is quite insensitive to the film thickness  $h$ , at least for  $h \leq 0.1\lambda$ . Finally in Fig. 4, the reflectivity and transmissivity for a Teflon film  $3\lambda$  thick is shown; one may observe the characteristic behavior of the *s* wave used by [19] for the free space measurement of  $\epsilon_r$  and  $\tan \delta$  at 90 GHz.

## 2.2 Multilayer and composite materials

Figure 5 shows a stack of dielectric material on a arbitrary substrate, each layer having different thickness  $h$  and complex refractive index  $\hat{n} = n_r - ik$ . In the following

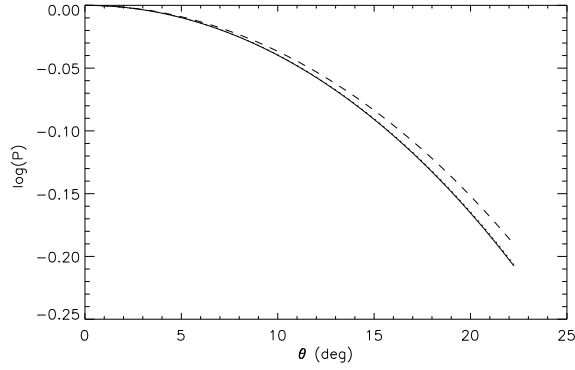


Figure 3: Ratio  $R_p/R_s$  versus the angle of incidence  $\theta$  for three Teflon film thickness:  $h = 0.01\lambda$  (solid),  $h = 0.025\lambda$  (dotted),  $h = 0.25\lambda$  (dashed)

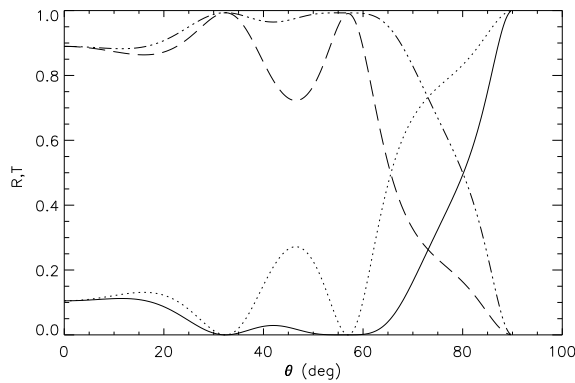


Figure 4: Reflectivity and transmissivity of a Teflon film  $3\lambda$  thick for  $p$  (solid - dash-dot-dot) and  $s$  (dotted - long dashes) polarization.

discussion, for simplicity, it is assumed normal incidence and  $n_0 = 1$ ,  $k_3 = 0$ <sup>1</sup>.

The structure basically operates as an optical coating in which constructive and destructive interference between rays emerge out after multiple internal reflections from various interfaces. For such a structure the method presented in the previous Section will rapidly become very cumbersome with the increase of the number of layers; it is much more convenient to use the characteristic matrix approach widely used in optical thin film analysis and synthesis [9]. A rigorous derivation of the method can be found in [6].

Let consider the first layer delimited by the interfaces  $a$  and  $b$  in Fig. 5, it can be shown [13, 9] that  $E_a$  and  $H_a$  are related to  $E_b$  and  $H_b$ , the tangential components of the electric  $\mathbf{E}$  and magnetic  $\mathbf{H}$  fields at  $a$  and  $b$ , by:

$$\begin{bmatrix} E_a \\ H_a \end{bmatrix} = \mathbf{M}_1 \begin{bmatrix} E_b \\ H_b \end{bmatrix} \quad (1)$$

with

<sup>1</sup>It is worth noting that at least for receiver installed in the secondary focus of a Cassegrain antenna, the beam, at few centimeters from the corrugated horn aperture, where the vacuum window is located, is fairly collimated. In these cases the normal incidence assumption is a quite good approximation.

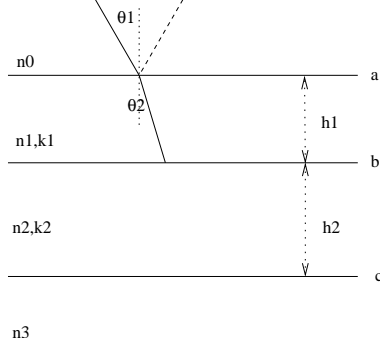


Figure 5: Stack of two dielectrics on a substrate

$$\mathbf{M}_1 = \begin{pmatrix} \cos \delta_1 & (i \sin \delta_1)/\hat{y}_1 \\ i \hat{y}_1 \sin \delta_1 & \cos \delta_1 \end{pmatrix} \quad (2)$$

where  $\delta_1 = 2 \pi \hat{n}_1 h_1/\lambda$  is the phase thickness,  $\hat{n}_1$  the complex refractive index,  $h_1$  the film thickness,  $\lambda$  the wavelength and  $\hat{y}_1$  the characteristic optical admittance of the medium

Furthermore, defining  $\hat{Y} = H/E = \hat{n}Y_0$  as the characteristic optical admittance of a medium with complex refractive index  $\hat{n}$ ,  $\hat{Y}_0 = (\epsilon_0/\mu_0)^{0.5}$  being the free space optical admittance, one can write the Eq. (1) as:

$$\begin{bmatrix} E_a \\ H_a \end{bmatrix} = E_a \begin{bmatrix} 1 \\ \hat{Y} \end{bmatrix} = \begin{bmatrix} B \\ C \end{bmatrix} E_b$$

with

$$\begin{bmatrix} B \\ C \end{bmatrix} = \mathbf{M}_1 \begin{bmatrix} 1 \\ \hat{y}_2 \end{bmatrix} \quad (3)$$

The layer is then equivalent to a single interface with an input optical admittance  $\hat{Y} = C/B$ . The reflection coefficient of such a system can be simply written [20]

$$\mathcal{R} = \frac{Y_0 - \hat{Y}}{Y_0 + \hat{Y}} = \frac{Y_0 B - C}{Y_0 B + C} \quad (4)$$

where  $Y_0$  is the optical admittance of the input medium, normally the free space.

Using the value of the transmitted power at the  $b$  interface  $P_t = 0.5Re(E_b H_b^*)$  and the incident power  $P_i = 0.5Re(E_a H_a^*)/(1 - \mathcal{R}\mathcal{R}^*)$  in  $a$ , the transmissivity  $T$  and the absorption  $A$  can be evaluated in terms  $Y_0, \hat{y}_2, B$  and  $C$  as [13]:

$$R = \mathcal{R}\mathcal{R}^* \quad (5)$$

$$T = \frac{4Y_0Re(\hat{y}_2)}{(Y_0 B + C)(Y_0 B + C)^*} \quad (6)$$

$$A = 1 - R - T \quad (7)$$

where for a single free standing layer,  $Y_0 = y_2 = 1$ .

The above equations can be generalized for an arbitrary stack of  $n$  dielectric layers on a generic substrate as sketched, for instance, in Fig. 5, by substituting Eq. 1 and 3 with, respectively,

$$\begin{bmatrix} E_a \\ H_a \end{bmatrix} = \prod_{i=0}^n \mathbf{M}_i \begin{bmatrix} E_n \\ H_n \end{bmatrix}$$

and

$$\begin{bmatrix} B \\ C \end{bmatrix} = \prod_{i=0}^n \mathbf{M}_i \begin{bmatrix} 1 \\ \hat{y}_{n+1} \end{bmatrix}$$

where  $\mathbf{M}_i$  are the characteristic matrices of each layer defined in Eq. 2 and  $\hat{y}_{n+1}$  the optical admittance of the last medium.

The multilayer is than equivalent to a single interface which has an input optical admittance  $\hat{Y} = C/B$ . The reflectivity, transmissivity and absorption can be evaluated with the above Eq. 4,7 and by substitution of  $\hat{y}_2$  with  $\hat{y}_{n+1}$  where for free standing stack, the case we are interested in,  $Y_0 = y_{n+1} = 1$ .

Summarizing, the procedure of finding  $R$  and  $T$  involves the knowledge of the optical admittances of the first  $Y_0$  and last medium  $\hat{y}_{n+1}$  and the computation of the stack equivalent optical admittance  $\hat{Y}$ .

The very interesting aspect of this approach is the possibility to analyze very complicated combination of different thickness and different materials by simply multiplying in the right order the characteristic matrices, the resulting one describing the whole system. It is worth noting that changing the order of multiplication one can evaluate the optical performances of a complicated system from both side; as matter of fact, as demonstrated by [1], while the transmittance is an invariant, the reflectivity, for non simmetric structures, will depend from the side we are looking at.

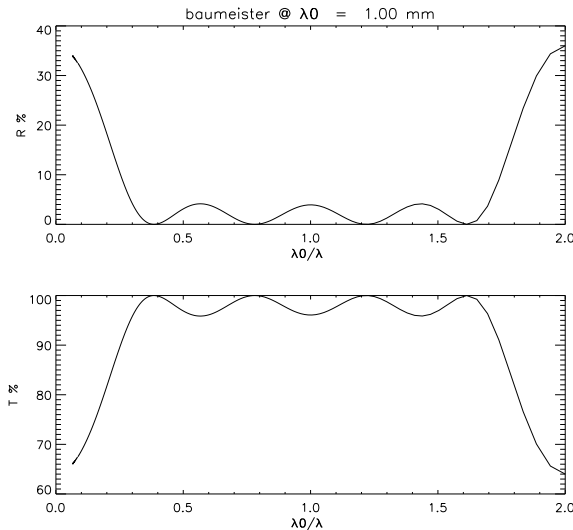


Figure 6: Reflectance and transmittance of five layers (from [4])

A simple IDL procedure, which can be easily translated in other languages, has been implemented to evaluate the reflectivity and transmissivity of an arbitrary array

of lossy dielectrics at normal incidence. The procedures presented so far have been tested with different combinations of refraction indices and thickness as found in the literature. For instance in Fig. 6 the results reported by [4] on five layers antireflection coating with Chebyshev response is reproduced with a high degree of accuracy. The same level of accuracy has been obtained in the reproduction of the reflectivity and transmissivity frequency response, evaluated with MMICAD software, of the 5 layers vacuum window proposed for millimetric ALMA receivers [11].

It is worth noting that multilayer structures can be analyzed also recurring to numerical techniques, that is the *Mode Matching* (MM) in its *Generalized Scattering Matrix* approach and the *Finite Element Method* (FEM).

MM is the numerical technique most close to analytical approaches, like the one here presented, due to its formulation making use of the field expansion into entire domain eigenfunctions. MM is best suited to analyze stacks of dielectric layers in waveguide, here successfully adopted to characterize electromagnetic parameters of dielectrics, since the excitations of higher order modes can be easily taken into account.

On the other hand FEM doesn't make use of any analytical solution of geometrical sub-parts of the domain to analyze: it is fully numerical from this point of view. It is based on the decomposition of the geometry to be analyzed in small volumes or elements where the electromagnetic field is described by simple functions. Than boundary conditions and excitations are imposed locally to allow, by means of a weight residual method, to get the solution. Its main feature is the ability to analyze any sort of electromagnetic problem and is particularly suited for complex geometries involving general shapes. An introductory description of both MM and FEM can be found for example in [10].

### 3 Optical performances of multilayer

We reports in this section  $R$  and  $T$  of some multilayers which could be used for large vacuum windows. The mechanical and electromagnetic parameters for some materials are reported in Appendix B. In the following example the characteristics of a window for a 4 - 8 GHz band phased array receiver [22] is shown. The window is a composite structure made by a 30 mm thick sheet of Rohacell WF51 both side coated with 0.2 mm film of NARMCO fiberglass glued with Araldite 106 as sketched in Fig. 7.

Figure 8 shows the responses for the three cases described in Table 1; the agreement with the results obtained using MM and FEM methods [15], despite the computational simplicity of the matrix method, is impressive.

As a second example,  $R$  and  $T$  in the 4 - 50 GHz band of a thermal filter made by a 0.15 mm thin black polyethylene enclosed between two 1.7 mm thick foils of Eccostock PP4 [25] is reported in Fig. 9 (dotted line). For comparison in the same figure the performances of the black polyethylene (solid line) and PP4 alone (dashed line) are reported. The thermal filtering properties of such materials will be the subject of a forthcoming paper.

Finally, it must be emphasized the availability of low loss new materials, like for instance Eccostock SH and Eccostock FPH [25], which can be obtained with dielectric constant ranging from 1.04 up to 1.25, usefull for very low reflectivity large bandwidth matching layers in the millimeter region.

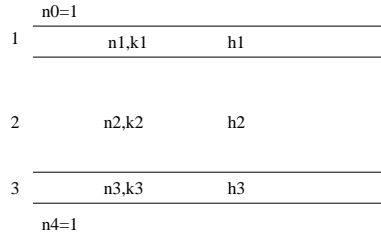


Figure 7: Free standing multilayer

Layer No.	Material	Thickness (mm)			$\epsilon_r$	$\tan \delta$
		case 1	case 2	case 3		
1	Glued Fiberglass*	0.38	0.38	0.5	4	0.02
2	Rohacell WF51	30	57	57	1.07	0.003
3	Glued Fiberglass	0.38	0.38	0.5	4	0.02

\* NARMCO preformed fibreglas + Araldite 106

Table 1: Details of multilayer window

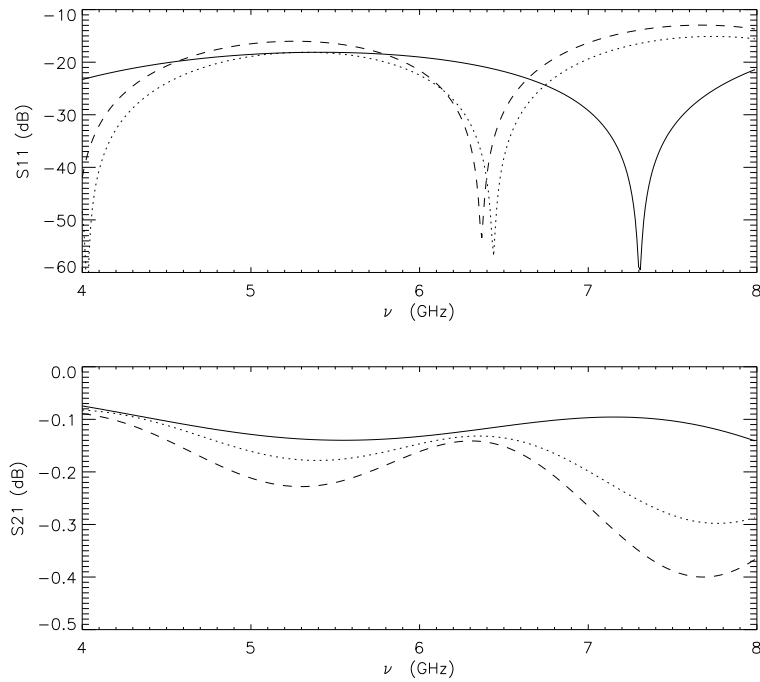


Figure 8: Frequency response of a multilayer. With reference to Table 1, *continuous line* case 1, *dotted* case 2 and *dashed* case 3

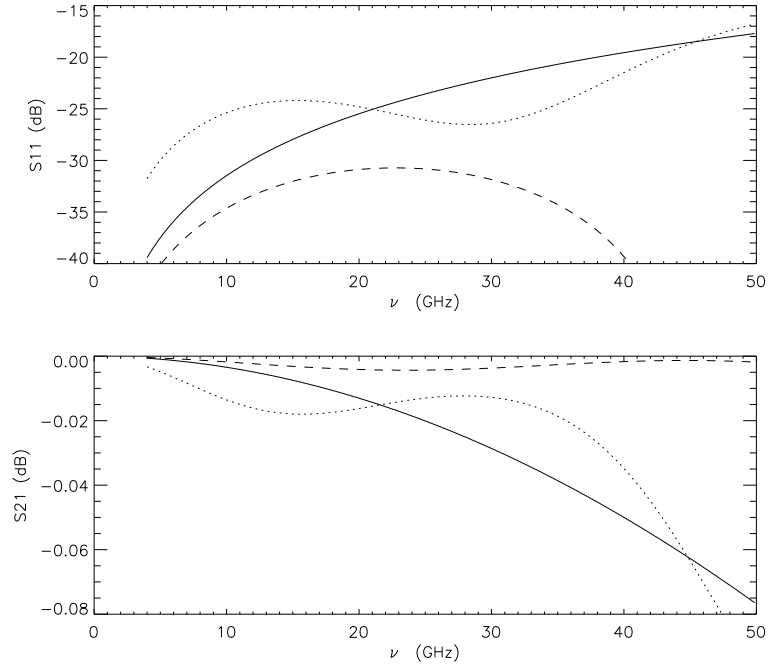


Figure 9: Frequency response of a multilayer thermal filter. Black polyethylene 0.15mm thick (*solid*), 1.7 mm of Eccostock PP4 (*dashed*) and a 0.15mm thick black Poly between two PP4 foils 1.7 mm thick (*dotted*)

## 4 Conclusions

Two simple computation techniques of easy implementation on a variety of programming languages for the evaluation of vacuum windows optical performances have been described. Performances obtainable from some multilayers are simulated.

The method could be also applied to the analysis of thermal multiple filtering, i.e. when several filters at the same or at different temperatures are used to minimize the thermal load on a cryogenerator. In this last case, however, one has to be very careful with the interpretation of the results because of non parallelism between the material layers.

## References

- [1] Abelés, F., *Ann. d. Physique*, **3**, 504, 1948
- [2] Afsar, M.,N, and Button,K.,J., *Proc. of the IEEE*, **73**, 131, Jan., 1985
- [3] Amitabha Basu, B. S. Verma, M. Kar, R. Bhattacharyya, and V. V. Shah, *Appl. Opt.*, **27**, 3362, 1988
- [4] Baumeister, P., *Appl. Opt*, **25**,4568, 1986
- [5] Birch, J., R., *Infrared Phys.*, Vol.**33**, pp. 33, Jan. 1992
- [6] Born & Wolf, *Principles of Optics*, Pergamon Press, 1975, Chap. 1.
- [7] Born & Wolf, *Principles of Optics*, Pergamon Press, 1975, Chap. 7.
- [8] Goldsmith, P.F., *Quasioptical Systems*, IEEE Press, 1998
- [9] Heavens, O.S., *Optical properties of thin solid films*, Butterworths Scientific Publications, London, 1955
- [10] Tatsuo Ithoh, *Numerical techniques for microwave and millimeter-wave passive structures*,John Wiley & Sons, 1988
- [11] Koller,D., Kerr A.R., Ediss, G.A., Boyd, D., *Alma Memo*, **377**, June,2001
- [12] Lamb,J.W.,*Int. J. Infrared Millimeter Waves*, **17**,Dec. 1996, pg.1997
- [13] Macleod,H.A., *Thin-film optical filters*, Adam Hilger Ltd, Bristol, 1986
- [14] Murray, A.G., *Infrared Phys.*, **33**, 113, 1992.
- [15] Natale, V., Nesti, R., "PHAROS dewar vacuum window", PHAROS document, July 2005
- [16] Nesti, R., Natale, V., "Notes on Dielectric Characterization in Waveguide", *SRT Report*, May 2005
- [17] Padman, R., *IEEE Trans. Antennas Propagat.*, **AP-26**, 741, Sept. 1978
- [18] Raguin,D.,H., Morris,G.M., *Appl. Opt.*, **32**, 1154, March 1993
- [19] Shimabukuru, F.,I., Lazar, S., Chernick, M. R., Dyson, H., B., *IEEE Trans. Microwave Theory Tech.*, **MTT-32**, pg. 659, July 1984
- [20] John C. Slater and Nathaniel H. Frank, "Electromagnetism", Dover Publications, Inc, New York, 1969
- [21] A. F. Turner and P. W. Baumeister, *Appl. Opt* **5**, 69 (1966).
- [22] Pharos project (<http://www.pharos-eu.org>)
- [23] Basf (<http://www.basf-italia.it>)
- [24] Degussa (<http://www.rohacell.com/en/performanceplastics.html>)
- [25] Emerson & Cuming (<http://www.eccosorb.com>)

## A Derivation of $n$ and $\tau$ from $\epsilon$ and $\tan \delta$

In this section the relationships between the electromagnetic quantities  $\epsilon$  and  $\tan \delta$  with the refractive index  $n$  and the absorption coefficient  $\tau$  are reported for non-conducting media. For absorbing media the complex wavenumber  $\hat{\mathbf{k}}$  can be written in way formally identical with the correspondig relation for ideal non-absorbing media if in the latter the dielectric constant is replaced by a complex quantity  $\hat{\epsilon}$ :

$$\hat{\mathbf{k}} = \frac{\omega}{c} \sqrt{\mu_r \hat{\epsilon}_r} \quad \hat{\epsilon}_r = \epsilon' + j\epsilon'' \quad \tan \delta = \frac{\epsilon''}{\epsilon'}$$

where  $\omega = 2\pi\nu$ ,  $\nu$  the frequency,  $\mu_r$  the relative magnetic permeability,  $\hat{\epsilon}_r$  the complex relative dielectric constant, and  $\epsilon_0$  is the vacuum dielectric constant. It is worth noting that both  $\epsilon'$  and  $\epsilon''$  can be assumed as constants only for  $\nu$  quite far from resonant frequencies of the medium.

Continuing with the analogy with ideal non-absorbing media, in addition to  $\hat{\mathbf{k}}$  and  $\hat{\epsilon}_r$ , also a complex phase velocity  $\hat{v}$  and refractive index  $\hat{n}$  can be defined and for which are still valid the following relations:

$$\hat{v} = \frac{c}{\sqrt{\mu_r \hat{\epsilon}_r}} \quad \hat{n} = \frac{c}{\hat{v}} = \frac{c}{\omega} \hat{\mathbf{k}} = \sqrt{\mu_r \hat{\epsilon}_r}$$

Going on with the analogy, the complex refractive index  $\hat{n}$  may be defined as

$$\hat{n} = n + j\kappa$$

where  $n$  is the real refractive index and  $\kappa$  the extinction coefficient. The connection between  $\epsilon_r$ ,  $\tan \delta$  and  $n$ ,  $\tau$  can be obtained by the relation  $\hat{n}^2 = \mu_r \hat{\epsilon}_r$ ; equating the real and imaginary parts and assuming  $\mu_r = 1$  (always valid for dielectrics) we can write:

$$n^2 - \kappa^2 = \epsilon' \quad \text{and} \quad 2n\kappa = \epsilon''$$

With simple algebra one can write the following explicit relationships:

$$n = (0.5 \epsilon_r \xi)^{0.5} \quad \kappa = \frac{\tan \delta \sqrt{\epsilon_r}}{(2 \xi)^{0.5}}$$

with  $\xi = 1 + \sqrt{1 + \tan^2 \delta}$ .

Lets now recall the simplest solution of the electromagnetic wave equation, i.e. a plane wave of unit amplitude travelling in the  $x$  direction  $\mathbf{E} = e^{i(\hat{\mathbf{k}}x - \omega t)}$ . Using the definition of  $\hat{\mathbf{k}}$  and simple algebra we obtain the energy density inside the medium:  $\simeq e^{-\tau x}$  with  $\tau$  the attenuation coefficient given by:

$$\tau = \frac{2\omega}{c} \kappa = \frac{2\pi}{\lambda_0} \frac{1}{n} (2n\kappa) = \frac{2\pi}{\lambda_0} \frac{1}{n} \epsilon'' \quad (\text{Neper/cm})$$

which is the relationship between the absorption coefficient and the material electromagnetic constants. For good dielectrics ( $\kappa \ll n$ ,  $\epsilon'' \ll \epsilon'$ ) we finally obtain the well known relationships:

$$n = \sqrt{\epsilon'} \quad \kappa = 0.5 n \tan \delta \quad \tau = \frac{2\pi}{\lambda_0} n \tan \delta \quad (\text{Neper/cm})$$

where  $\lambda_0$  is the vacuum wavelength expressed in  $cm$ .

## B Mechanical and electrical properties

Material	Tensile Modulus (GPa)	Tensile Strength (MPa)	Poisson's Coeff.	$\nu$ (GHz)	$\epsilon$	$\tan\delta \times 10^{-4}$
LDPE	0.1-0.3	5-25	-	26-38	2.302	3.8
HDPE	0.5-1.2	15-40	0.5	35	2.36	1.7
Polypropylene	0.9-1.5	25-40	-	35	2.25	1.55
Polystyrene (PS)	2.3-4.1	30-100	0.35	26-38	2.56	8.7
Rexolite (cross linked PS)	1.65	55-70	-	26-38	2.55	8.9
Teflon PTFE	0.3-0.8	10-40	0.46	26-38	2.1	2.17
TPX	1.5	25	-	34.5	2.126	4.8
Plexiglas	2.4	80	0.35-0.4	3.75-12.5	2.5	41
				19-26	2.54	45
				50	2.56	32
Mylar (PETP) <sup>1</sup>	2 - 4	80	0.37	55	3.145	44
Kapton <sup>2</sup>	2 - 3	70 - 150				

<sup>1</sup> Polyethylene terephthalate, <sup>2</sup> Polyimide

Table B.1: Mechanical and electrical properties of some plastics used for vacuum windows

Material	Frequency (GHz)	$\epsilon_r$	$\tan\delta(x10^{-4})$
Rohacell 31 HF	18 - 26	1.056	16
51 HF	"	1.07	20
71 HF	"	1.1	29
51 WF	"	1.07	29
Styropor PS30SE	"	1.046	0.7
NARMCO 3203 7781*	"	4	190
Styrodur 4000Cs	3.75 - 6.25	1.034	$\leq 1$
	7.5 - 12.5	1.04	$\leq 1$
	18 - 26	1.07	0.3
Eccostock PP2	$\leq 10$	1.03	1
PP4	"	1.06	1
LoK (rigid)	"	1.7	4
Black cardboard	5 - 8	3.8	200
	18 - 26		
Black polyethylene	5 - 8	2.7	10
	18 - 26	2.7	10

<sup>1</sup> preformed fiberglass

Table B.2: Electrical properties of some foams

Material	Density $kg/m^3$	Compressive Elastic modulus (MPa)	Tensile strength (MPa)	Compressive strength (MPa)	Shear modulus (strength)(MPa)
Rohacell 31 HF	32	36	1.0	0.4	13 (0.4)
51 HF	52	70	1.9	0.9	19 (0.8)
71 HF	75	92	2.8	1.5	29 (1.3)
51 WF	51	72	1.6	0.3	16 (0.6)
Styropor PS30SE	30	8 - 11.5	0.4		
NARMCO 3203 7781 <sup>1</sup>		26000*	483		
Styrodur 2800C	30	15			( $\leq 0.3$ )
4000CS	45	30			( $\leq 0.3$ )

<sup>1</sup> preformed fiberglass,\* Young's module

Table B.3: Mechanical properties of some foams